Age-dependent divergent interactions between CX3CR1 absence and MK- 801 neonatal administration in a novel “dual hit” schizophrenia model

Felipe A. Méndez
Universidad Nacional Autónoma de México
Mayra Itzel Torres-Flores
Universidad Nacional Autónoma de México
Benito Ordaz
Universidad Nacional Autónoma de México
Fernando Peña-Ortega (jfpena@unam.mx)
Universidad Nacional Autónoma de México

Research Article

Keywords: MK-801, dizocilpine, microglia, fractalkine, schizophrenia, epilepsy

Posted Date: March 27th, 2023

DOI: https://doi.org/10.21203/rs.3.rs-2719057/v1

Abstract

The diathesis–stress model of schizophrenia posits that a constitutive factor increases the vulnerability to secondary stressors. Alterations in neuron–microglia communication through the fractalkine pathway is a potential predisposing factor. Wild-type (WT) and *Cx3cr1*$^{-/-}$ (KO) mice of both sexes randomly received either a low (0.5 mg/kg) or high dose (1 mg/kg) of MK-801 or saline during early postnatal development. Neuronal apoptosis was assessed at a midpoint of the pharmacological protocol. Survival and growth rates were determined up to adulthood when innate behaviors, unconditioned anxiety, contextual memory and seizure susceptibility were evaluated, as well as hippocampal local field potential and sensory gating. Fractalkine receptor (CX3CR1) depletion and MK-801 treatment had a synergistic effect, increasing neuronal apoptosis and overall mortality. Both factors independently induced long-lasting cognitive impairments in the wide array of tasks assessed. Low MK-801 dose treatment greatly augmented the mortality of pentylenetetrazol-induced seizures in WT mice, an effect prevented by CX3CR1 depletion. MK-801 treatment induced a shift in the power spectrum of the hippocampal local field potential towards higher frequencies that was averted in *Cx3cr1*$^{-/-}$ mice by an opposite shift. CX3CR1 depletion severely increases the vulnerability to neonatal NMDA antagonism with additional complex interactions regarding cognitive and neurophysiological effects.

Introduction

Schizophrenia etiology and physiopathology remain largely unknown, hindering the development of appropriate treatments (Braff & Braff, 2013; Miyamoto et al., 2005; Murray et al., 2017). The multifactorial nature of schizophrenia has been addressed by dual-hit or diathesis–stress models, whereby individuals present a predisposition that primes them for the development of psychotic disorders upon exposure to a secondary factor such as stress (Howes et al., 2017), drug abuse (Nakazawa et al., 2017) or immune activation (Feigenson et al., 2014; Howes & McCutcheon, 2017). Microglia have recently been recognized as a potential key element in this disorder, based on evidence of neuroinflammation (Fries et al., 2018; Goldsmith et al., 2016; Mongan et al., 2019; Réus et al., 2015) and microglial activation (Bloomfield et al., 2016; Inta et al., 2017; van Berckel et al., 2008) in patients with schizophrenia.

A major communication axis between microglia and neurons is the fractalkine pathway (Arnoux & Audinat, 2015), which is involved in circuit refinement during development (Paolicelli et al., 2011) and the brain's response to environmental stressors (Cardona et al., 2006; Eyo et al., 2016; Milior et al., 2016; Pagani et al., 2015). The targeted interruption of this pathway, through the depletion of either fractalkine(Paolicelli et al., 2014) or its receptor (CX3CR1) (Jung et al., 2000; Yona et al., 2013), results in long-lasting alterations in microglia and synaptic physiology with cognitive and behavioral consequences (Méndez-Salcido et al., 2022; Paolicelli et al., 2011; Rogers et al., 2011; Zhan et al., 2014). The mechanisms involved include impaired neuronal survival (Ueno et al., 2013), synapse maturation (Zhan et al., 2014) and pruning (Paolicelli et al., 2011), and impaired microglial activation (Pagani et al., 2015). These alterations fit well within the neurodevelopmental (Howes et al., 2017; Murray et al., 2017; Owen et al., 2011), synaptic pruning (Feinberg, 1982; Keshavan et al., 1994; Sellgren et al., 2019), and

neuroinflammatory (Howes & McCutcheon, 2017; Inta et al., 2017; Mongan et al., 2019) hypotheses of schizophrenia (Howes & Shatalina, 2022). Neonatal blockage of NMDA (*N*-methyl-D-aspartate) receptors causes alterations during nervous system development, including neuronal apoptosis (Hansen et al., 2004; Ikonomidou et al., 1999), as well as long-term behavioral and cognitive impairments in the adult organism (Coleman et al., 2009; Lim et al., 2012), constituting the basis of the glutamatergic hypothesis of schizophrenia (Lee & Zhou, 2019; Lim et al., 2012; Nakazawa et al., 2017).

In the present study, we explore the interaction between the interruption of the fractalkine/CX3CR1 axis, by CX3CR1 depletion, and neonatal NMDA blockade regarding neurotoxicity, survival, behavior, and seizure susceptibility in a novel two-hit model of schizophrenia.

Materials And Methods

Animals and neonatal MK-801 treatment

Cx3cr1 $^{-/-}$ knockout (KO) mice (RRID:IMSR_JAX:025524) (Yona et al., 2013) were acquired from the Jackson Laboratory (Maine, USA), backcrossed with C57BL/6J wild-type (WT) mice, and housed under a standard 12 h light/dark cycle, with controlled temperature (24ºC) and food and water *ad libitum*.

Pups were carefully sexed, weighted and randomly assigned on postnatal day 5 (PD5) to receive either a low (0.5 mg/kg) or high (1 mg/kg) intraperitoneal (IP) dose of MK-801 (Sigma, Missouri, USA), or an equivalent volume of saline (NaCl 0.9%), every 24 h for five consecutive days (PD5-9) (Coleman et al., 2009; Fredriksson & Archer, 2004).

All subjects were weighted daily from PD5 to PD35 and every fifth day afterwards until PD90. For survival curves, death was considered to be related to the treatment if it occurred during the pharmacological protocol or up to a week after and only if the subject presented arrest in development or other signs of deterioration previous to its demise.

Survival curves were fitted with the Kaplan–Meier model and pairwise comparisons among groups were carried out with the log-rank test followed by a Bonferroni correction for multiple comparisons (Table 1). Growth was compared among groups at PD5, PD10, PD50 and PD90 with a mixed model ANOVA followed by a multiple t-test with Holm correction.

Table 1
Pairwise log-rank tests for the survival curves in Fig. 1. *p* values were adjusted with the Bonferroni correction for multiple comparisons. KO: *Cx3cr1*$^{-/-}$, WT: *Cx3cr1*$^{+/+}$

Group 1	Group 2	t	*p*	*p corrected*
KO-0.5mg/kg	KO-1mg/kg	61.65	4.1×10^{-15}	< 0.0001
	KO-Saline	8.47	3.6×10^{-3}	0.054
	WT-0.5mg/kg	1.2	2.7×10^{-1}	1.0
	WT-1mg/kg	0.13	7.2×10^{-1}	1.0
	WT-Saline	2.95	8.6×10^{-2}	1.0
KO-1mg/kg	KO-Saline	109.88	1.04×10^{-25}	< 0.0001
	WT-0.5mg/kg	52.44	4.44×10^{-13}	< 0.0001
	WT-1mg/kg	30.73	2.96×10^{-8}	< 0.0001
	WT-Saline	66.56	3.39×10^{-16}	< 0.0001
KO-Saline	WT-0.5mg/kg	2.84	9.17×10^{-2}	1.0
	WT-1mg/kg	9.78	1.76×10^{-3}	0.02
	WT-Saline	1.05	3.06×10^{-1}	1.0
WT-0.5mg/kg	WT-1mg/kg	1.62	2.02×10^{-1}	1.0
	WT-Saline	0.37	5.44×10^{-1}	1.0
WT-1mg/kg	WT-Saline	3.55	5.93×10^{-2}	0.89

Nissl Staining

Apoptosis was assessed by the presence of pyknotic bodies in Nissl-stained sections (Salgado-Puga et al., 2015; Tapia et al., 1999). Briefly, the treatment was interrupted at the third administration. Twenty-four hours later, the pups were anesthetized with 2% sevoflurane, decapitated, and the brains were fixed overnight in 4% paraformaldehyde (Sigma, USA) in phosphate-buffered saline (PBS; Sigma, USA). Cryosections (30 µm thick) were obtained (CM 350S, Leica, Wetzlar, Germany) from the prefrontal cortex up to the dorsal hippocampus, mounted on gelatinized slides, stained with Nissl (Paul et al., 2008; Van Eden & Uylings, 1985) (0.1% cresyl violet, Sigma, USA) and coverslipped with DPX medium (Sigma, USA).

Bright-field photomicrographs were obtained with 10X and 40X magnification and 2048 x 1538 pixel resolution (DMC5400, Leica, Germany) of frontal cortical and striatal regions. Pyknotic bodies were semi-manually quantified per 40X field with FIJI software (RRID:SCR_002285) and its CellCounter plug-in (Schindelin et al., 2012). Pyknotic cells per field were compared among groups by a two-way ANOVA followed by the Tukey–HSD test.

Behavioral Phenotyping

Behavioral tests were performed with adult mice (16–48 weeks old) of both sexes in the following order to minimize the effect of stressful tasks: nesting, burrowing, open field, y-maze and passive avoidance test (Bell, 2013; McIlwain et al., 2001).

Nesting

Nesting was assessed following previous protocols (Deacon, 2012; Deacon, 2006a). Briefly, the test was performed 48 h after habituation to the nesting material (5x5 cm square cotton pads) with subjects placed individually in cages with new bedding and a cotton pad at the beginning of the dark phase of their cycle. Nesting was scored the next morning according to Deacon's scale (Deacon, 2012; Deacon, 2006a) and compared with the Kruskal–Wallis test, followed by Dunn's *post hoc* test.

Burrowing

Burrowing behavior was assessed according to previous protocols (Deacon, 2012; Deacon, 2006b). A baseline test was performed placing the mice individually in clean cages containing a burrow filled with 400 g of small river gravel (0.5-2 cm) overnight (Deacon, 2006b). This procedure was repeated 48 h later. Gravel remaining in the burrow was weighted in the morning and subtracted from the initial weight. Comparison among groups was assessed with the Welch ANOVA test followed by the Games–Howell *post-hoc* test.

Open Field

The open field test was performed with the SuperFlex Open Field automated system (Omnitech Electronics, Ohio, USA). Horizontal (ambulation) and vertical (rearing) activity was automatically detected and analyzed by Fusion software (Omnitech Electronics, RRID:SCR_017972). Total distance travelled, accumulated immobility time, percentage of time in the center of the arena and the number of vertical rearings were compared among groups (Seibenhener & Wooten, 2015) with the ANOVA test followed by the Tukey–HSD *post hoc* test when appropriate.

Y maze

The spontaneous alternation task in the Y maze was carried out in a custom-made light gray acrylic apparatus. Each subject was individually placed at the end of one of the arms and left to explore freely

for 10 min. The videotape was later analyzed with SMART software (v. 3, Panlab, Harvard Apparatus, Barcelona, Spain, RRID:SCR_002852).

Total distance explored, number of entries into each arm, number of successful full alternations, and the percentage of full alternations were quantified (Kraeuter et al., 2019) and compared among groups by the ANOVA test followed by the Tukey–HSD *post hoc* test.

Passive Avoidance Test

The passive avoidance test was performed in an apparatus that consists of two chambers, one illuminated and the other one kept dark and equipped to deliver a 0.1 mA (5 s long) electric shock.

One day after habituation to the apparatus, animals were placed in the illuminated chamber and, 30 s later, allowed to enter the dark chamber where the electric shock was delivered (Salgado-Puga et al., 2015; Venable & Kelly, 1990).

The acquisition of the association was assessed 2 h later, repeating the same procedure and quantifying the latency to cross to the dark chamber with a maximum limit of 300 s. Memory retrieval was assessed in a similar manner 24 h later (Salgado-Puga et al., 2015; Venable & Kelly, 1990). The latencies to enter into the dark chamber during the conditioning and acquisition phases (2 h test) were compared with a mixed model ANOVA test followed by a pairwise t-test with Holm correction, while the latencies during the retrieval phase (24 h test) were compared among groups with the Kruskal–Wallis test followed by the Dunn test.

Electrophysiological recordings

In vivo electrophysiological recordings of both spontaneous activity and evoked auditory potentials were acquired from the dorsal hippocampus of mice under urethane (1.3–1.5 g/kg IP; Sigma, USA) anesthesia following previous protocols (Clement et al., 2008; Dissanayake et al., 2008). Briefly, anesthetized animals were mounted in a stereotaxic frame (#51500U, Stoelting, Illinois, USA). A craniotomy was performed through which a 32-channel, multi-shank silicon probe (A4x8-5mm-200-400-177, Neuronexus, Michigan, USA) was slowly inserted (the medial most shank reached the following coordinates from Bregma: -2 mm anteroposterior, 1.3 mm lateral and − 2.3 mm ventral), allowing the simultaneous recording of the major regions of the dorsal hippocampus (Cornu Ammonis 1, CA1; Cornu Ammonis 3, CA3; and Dentate Gyrus, DG) (Montgomery et al., 2008). Previous to insertion, the tracer DiI (1,1'-Dioctadecyl-3,3,3',3'-Tetramethylindocarbocyanine Perchlorate, Invitrogen, USA) was applied to the silicon probes to track the recording site (Méndez-Salcido et al., 2022). Broadband (0.28 Hz – 7.6 KHz) electrophysiological signals were amplified and digitized at 25 KHz (RHD2000 Interface Board, RHX Data Acquisition Software, Intan Technologies, California, USA, RRID:SCR_019278).

After a 30 min stabilization period, spontaneous activity was recorded from all channels for 30 min, followed by the recording of 140 trials of hippocampal auditory potentials evoked by paired 3 KHz, 20 ms long tones with a 0.5 s interval (Dissanayake et al., 2008; Krause et al., 2003; Miller & Freedman, 1995, p.

3) synthetized in Matlab (MathWorks, Massachusetts USA, RRID:SCR_001622), triggered every 10 s by a pulse generator (Master-8, AMPI, Jerusalem, Israel). The probe was removed and the brain was dissected and sliced (HM 650V, Thermo Scientific, Massachusetts, USA) for histological verification of the recording site.

One channel was selected per region of the hippocampus for spectral analysis of the local field potential (LFP), which was performed in one-minute-long periods of spontaneous activity, low-pass filtered (350 Hz), and down-sampled (1 KHz) using two-second-long windows with no overlap using a Hanning window. Relative power of delta (< 3 Hz), “urethane theta” (Kramis et al., 1975; Peña et al., 2010; Vandecasteele et al., 2014) (3–6 Hz), and low gamma (30–50 Hz) were calculated from Welch periodograms. A multivariate analysis of variance (MANOVA) was carried out with the relative power of the three bands (delta, theta and low gamma) as dependent variables and recording site (hippocampal region), pharmacological treatment, and genotype as independent variables. Significant results were followed by two- or three-way ANOVA tests, as appropriate, with alpha adjusted by the number of independent variables.

Auditory evoked potentials were similarly filtered and the channel with best signal-to-noise ratio in the CA3 region was chosen for further analysis(Adler et al., 1986; Dissanayake et al., 2008). The equivalent of P20 and N40 were determined in order to obtain the amplitude and latency of the conditioned stimulus (CAMP and CLAT, respectively) and test stimulus (TAMP and TLAT, respectively). An index of attenuation was calculated as the ratio of TAMP/CAMP (T/C) (Dissanayake et al., 2008; Krause et al., 2003).

Susceptibility and mortality to pentylenetetrazol-induced seizures

A dose-response curve for seizures induced by pentylenetetrazol (PTZ, Sigma, USA) was performed (Shimada & Yamagata, 2018; Van Erum et al., 2019). Mice of both sexes between 24 and 48 weeks old were treated IP with 20 mg/kg of PTZ, in saline, every 15 min until a total of 80 mg/kg was reached, while behavioral signs of seizures were evaluated following a revised Racine scale (Shimada & Yamagata, 2018; Van Erum et al., 2019). The highest severity reached with each dose was compared with a mixed model ANOVA test followed by a pairwise t-test with Holm correction. Mortality was compared with pairwise binomial tests followed by a Holm correction for multiple comparisons.

The effect of the different treatments on WT mice are presented first, followed by the comparison with similarly treated KO mice. Effect sizes are presented as Hedge’s g unless otherwise stated. Alpha level is $p < 0.05$ for all statistical tests, unless otherwise stated, and symbols in figures represent p values as follows: * < 0.05, ** < 0.01, *** < 0.001.

Results

CX3CR1 depletion increases MK-801 toxicity in neonatal mice

Mice of both genotypes (*Cx3cr1*$^{+/+}$ = WT, and *Cx3cr1*$^{-/-}$ = KO) were treated with a low (0.5 mg/kg) or high dose (1 mg/kg) of the non-competitive NMDA antagonist MK-801 or an equivalent volume of saline during postnatal days PD5-PD9. Surprisingly, the KO group treated with the high MK-801 dose (1 mg/kg) had a sharp increase in mortality, reaching over 90% by the end of the protocol, in striking contrast to its WT counterparts (Fig. 1A, Table 1). Accordingly, the high dose of MK-801 induced a large increase in neuronal apoptosis in the neocortex (WT-high dose vs high dose-KO; $p = 0.001$, Hedges' g = 2.13) and striatum (WT-high dose vs high dose KO; $p = 0.001$, Hedges' g = 1.22) of KO mice after only three administrations (Fig. 1E-F), suggesting a synergistic interaction between NMDA antagonism and CX3CR1 depletion in the acute toxicity of NMDA antagonism. Due to the low survival rate of this group, it was excluded from all other experimental procedures.

In WT mice, MK-801 administration induced a significant and dose-dependent delay in growth that was most prominent at the end of treatment (P10; WT-Saline vs WT-low dose Hedges' g = 0.92; WT-Saline vs WT-high dose Hedges' g = 2.44) and normalized in adulthood (Fig. 1B-C). The low MK-801 dose affected WT and KO mice similarly, inducing an equivalent delay in growth (similar effect size) during development compared to their respective controls (P10; WT-Saline vs WT-low dose Hedges' g = 0.92, KO-Saline vs KO-low dose Hedges' g = 0.89) (Fig. 1B, 1D).

Behavioral Phenotyping

Innate behaviors as potential indicators of negative symptoms

Negative symptoms of schizophrenia, such as avolition (Strauss et al., 2016), despite being regarded as central to the pathology (Strauss et al., 2021), remain poorly understood and lack a clear behavioral equivalent in model organisms, thus we performed an assessment of two innate behaviors—nesting and burrowing—considered sensible indicators of general well-being in rodents (Jirkof, 2014; Méndez-Salcido et al., 2022).

In WT mice, neonatal treatment with MK-801 had a dose-dependent effect on nest building (Fig. 2A *top*) with only the high dose having a significant effect (Dunn's test; WT-Saline vs WT-high dose, $p = 0.014$, Fig. 2A *Top*). We found similar results in KO mice, as the low MK-801 dose did not affect nesting significantly and no significant interaction between genotype and treatment was found, (Kruskal–Wallis test, $p = 0.26$, Fig. 2A *Bottom*).

A greater sensibility was achieved with the burrowing test. In WT mice both low and high MK-801 doses induced a significant decrease in the amount of burrowed material with similar effect sizes (Games-Howell test; WT-Saline vs WT-low dose $p = 0.001$, Hedges' g = 1.29, WT-Saline vs WT-high dose $p = 0.001$, Hedges' g = 1.12, Fig. 2B *Top*) indicating a possible floor effect. In KO mice, we found independent significant effects of genotype and treatment. While CX3CR1 depletion alone induced a moderate effect with respect to WT mice (Games–Howell test; WT-Saline vs KO-Saline, $p = 0.004$, Hedges' g = 0.97, Fig. 2B *Bottom*), the low MK-801 dose induced an equally large effect on both genotypes (Games–Howell test; WT-Saline vs WT-low dose, $p = 0.001$, Hedges' g = 1.30, WT-Saline vs KO-low dose, $p = 0.001$, Hedges' g =

1.40, Fig. 2B *Bottom*). Although no interaction between factors was found, we cannot rule out the possibility of a floor effect.

Cognitive and emotionality assessment

Memory function was assessed with the passive avoidance test (Venable & Kelly, 1990). All groups displayed an adequate acquisition of the contextual association as demonstrated by a significantly increased latency to cross to the dark chamber in the test 2 h after the foot shock (Fig. 2C *Top* and *Bottom*). However, MK-801 treatment affected the mnemonic function, tested 24 h later, in a dose-dependent manner with only the high dose (1 mg/kg) reaching a significant reduction in latency in WT mice (Dunn test; WT-Saline vs WT-high dose $p = 0.02$, Fig. 2C *Top*). In contrast, KO mice showed memory impairment dependent mainly on their genotype, as KO-Saline mice displayed a reduced latency to cross, in the 24 h test, compared to WT mice (Dunn test; WT-Saline vs KO-Saline, $p = 0.04$), which was consistent with previous reports(Rogers et al., 2011). This reduced latency was not worsened by the pharmacological treatment (Dunn test; WT-Saline vs KO-low dose, $p = 0.03$, Fig. 2C *Bottom*).

Emotional response to stress was assessed with the open field under bright illumination (100 lux) whereby both doses of the MK-801 treatment induced robust alterations in the exploratory behavior of WT mice, consistent with increased anxiety (Fig. 3A-C *Top*). Total distance was reduced comparably in WT mice with both doses of MK-801 (Tukey-HSD; WT-Saline vs WT-low dose $p = 0.001$, Hedges' g = 1.14, WT-Saline vs WT-high dose $p = 0.001$, Hedges' g = 1.21, Fig. 3A *Top*). Accordingly, time spent in the center of the arena was reduced with a modest increment in effect size dependent on the MK-801 dose (Tukey-HSD; WT-Saline vs WT-low dose $p = 0.02$, Hedges' g = 0.75, WT-Saline vs WT-high dose $p = 0.002$, Hedges' g = 0.95, Fig. 3B *Top*). Finally, rearing behavior was greatly reduced by both treatments with a large effect size (Tukey-HSD; WT-Saline vs WT-low dose $p = 0.001$, Hedges' g = -1.22, WT-Saline vs WT-high dose $p = 0.001$, Hedges' g = -1.47, Fig. 3C *Top*).

In KO mice we found similar effects where genotype was a significant factor independently of treatment (Fig. 3A-C *Bottom*). Total distance was reduced in both WT and KO groups treated with the low dose of MK-801 (Tukey-HSD; WT-Saline vs WT-low dose $p = 0.001$, Hedges' g = 1.23, WT-Saline vs KO-low dose $p = 0.001$, Hedges' g = 1.09, Fig. 3A *Bottom*). Time spent in the center of the arena was reduced by both factors independently with treatment inducing greater effects (Tukey-HSD; WT-Saline vs KO-Saline $p = 0.04$, Hedges' g = 0.58, WT-Saline vs WT-low dose $p = 0.03$, Hedges' g = 0.80, WT-Saline vs KO-low dose $p = 0.001$, Hedges' g = 1.02, Fig. 3B *Bottom*). Rearing behavior was affected in a similar and independent manner by both factors (Tukey-HSD; WT-Saline vs KO-Saline $p = 0.049$, Hedges' g = 0.58, WT-Saline vs WT-low dose $p = 0.001$, Hedges' g = 1.38, WT-Saline vs KO-low dose $p = 0.001$, Hedges' g = 1.46, Fig. 3C *Bottom*).

Working memory was assessed by the spontaneous alternation task in the Y maze. However, spatial exploration was affected in a such a way that precluded an unbiased assessment. Even under the considerably less stressful conditions of the Y maze (i.e., dim light and narrow arms), both saline and KO-low dose mice displayed a drastically reduced total distance compared with their WT counterparts

(Tukey-HSD; WT-Saline vs KO-Saline $p = 0.001$, Hedges' g = 0.96, WT-Saline vs KO-low dose $p = 0.001$, Hedges' g = 1.77, WT-low dose vs KO-low dose $p = 0.001$, Hedges' g = 2.07, Fig. 3D *left*), with genotype and treatment being significant factors while also having a significant interaction, further diminishing the exploration of KO-low dose mice as compared with their saline-treated counterparts (KO-Saline vs KO-low dose $p = 0.001$, Hedges' g = 0.82, Fig. 3D *left*).

Divergent effects on the spectral composition of hippocampal LFP

In WT mice each of the independent variables (site and treatment) contributed significantly to the variation in the relative power of the delta, theta and gamma bands of hippocampal LFP recordings (MANOVA; site: Wilks' lambda = 0.55, $p = 0.0001$; treatment: Wilks' lambda = 0.63, $p = 0.0003$, Fig. 4A-C, F).

Specifically, neonatal MK-801 administration induced a significant reduction in the relative power of the delta band, independently of the site of recording (Two-way ANOVA; treatment [$F(2) = 9.02$, $p = 0.0004$], Fig. 4F) in a non-linear dose-dependent manner with the maximum effect in the WT-low dose group (Tukey-HSD; WT-Saline vs WT-0.5mg/kg: $p = 0.001$, Fig. 4F) and a corresponding increase in the theta band, again specifically in the WT-low dose group (Tukey-HSD; WT-Saline vs WT-0.5mg/kg: $p = 0.0015$, WT-1mg/kg vs WT-0.5mg/kg: $p = 0.0148$, Fig. 4F), as well as in the gamma band (Two-way ANOVA; treatment [$F(2) = 7.27$, $p = 0.0016$], Fig. 4F), both independently of site. Concretely, neonatal blockade of NMDA receptors results in a long-lasting disruption of the spectral composition of the hippocampal LFP in adulthood with a broad shift of the power from slow frequencies towards faster ones.

In contrast, we found that CX3CR1 absence during development has an opposing effect to that of the MK-801 treatment. While treatment (Wilks' lambda = 0.62, $p = 0.0001$), genotype (Wilks' lambda = 0.74, $p = 0.0001$) and site (Wilks' lambda = 0.66, $p = 0.0001$) all contribute significantly to the relative power of the delta, theta and gamma bands, they do so independently and in differing directions (Fig. 4A-E and G). As with the WT mice, treatment with MK-801 diminished delta band power independently of genotype (Tukey-HSD; Saline vs 0.5mg/kg: $p = 0.001$, Fig. 4G), while genotype increased delta power (Tukey-HSD; KO vs WT: p = 0.0096, Fig. 4G) independently of treatment or recording site. Similarly, MK-801 treatment increased theta and gamma band power (Tukey-HSD; theta band Saline vs 0.5mg/kg: $p = 0.001$; gamma band Saline vs 0.5mg/kg: $p = 0.001$, Fig. 4G), while CX3CR1 absence diminished it (Tukey-HSD; theta band KO vs WT: $p = 0.0024$; gamma band KO vs WT: $p = 0.0087$, Fig. 4A-E and G).

Hippocampal auditory gating is preserved

Given the robust changes in LFP recordings, we assessed the integrity of the hippocampal sensory gating to auditory stimuli(Smucny et al., 2015). Unexpectedly, we found no changes in the test to conditioning response ratio (T/C) (Fig. 5A-B) or in the amplitude or latency of the responses to the auditory stimuli in any group (Fig. 5A-B), indicating an intact sensory gating.

CX3CR1 depletion prevents MK-801 induced increase in seizure susceptibility

We performed a dose-response curve to assess seizure susceptibility to the GABA antagonist PTZ (Shimada & Yamagata, 2018; Van Erum et al., 2019). As previously reported (Gorter et al., 1991; Pierson & Swann, 1991), neonatal administration of MK-801 increased the susceptibility to seizures in WT mice treated with the high dose of MK-801 (1 mg/kg), reaching seizures of higher severity with the lowest dose of PTZ (20 mg/kg) (Holm corrected T-test; WT-Saline vs WT-high dose with 20 mg/kg PTZ: $p = 0.001$, Fig. 5C). Comparing equally treated groups of both genotypes, we did not find any increase in severity of seizures in the dose-response curve as assessed by the modified Racine scale (Van Erum et al., 2019) (Fig. 5D).

Surprisingly, the WT-low dose mice had an important increase in mortality due to respiratory arrest or status epilepticus induced by the total dose of PTZ (80 mg/kg) (Binomial test with Holm correction: WT-Saline vs WT-0.5mg/kg, $p = 0.005$, WT-Saline vs WT-1mg/kg, $p = 1.0$, Fig. 5E) that is not observed in equally treated KO mice (WT-Saline vs KO-0.5mg/kg, $p = 1.0$, Fig. 5E).

Discussion

In the context of a diathesis-stress model (Howes & McCutcheon, 2017; Howes & Shatalina, 2022; Murray et al., 2017), our results present a complex interaction between CX3CR1 absence and neonatal NMDA receptor antagonism that ranges from synergistic interaction in acute toxicity, increasing neuronal apoptosis and overall mortality, to largely independent or additive effects in cognitive alterations in adulthood, to opposing effects in the spectral composition of hippocampal LFP and seizure susceptibility.

Considering that NMDA antagonism in the neonatal period induces an acute drop in neurotrophic factors leading to neuronal apoptosis (Hansen et al., 2004; Heck et al., 2008; Ikonomidou et al., 1999) and that microglia plays an important role in neuronal survival in normal development (Ueno et al., 2013), as well as in pathologic conditions (Bessis et al., 2007; Inta et al., 2017), we argue that the disruption of the fractalkine pathway impairs the microglial response to neuronal stress, further diminishing trophic support and thus contributing to widespread neuronal death. This synergy suggests that CX3CR1 absence induces a window in early development of exquisite vulnerability to environmental factors, such as NMDA antagonism, supporting its potential as a diathetic element.

We found long-term behavioral consequences arising from CX3CR1 absence and/or NMDA blockade, largely independently, affecting innate behaviors, contextual memory, emotionality, and spatial exploration. Contextual memory and anxiety-like behavior were primarily affected by CX3CR1 absence, with little added effect by the NMDA blockade, overall severely disrupting exploratory behavior. To our knowledge this is the first work addressing innate behaviors in the neonatal NMDA blockade model; both tasks assessed here were affected by treatment as well as by CX3CR1 absence. Since these behaviors directly attend to primary needs and are already studied as correlates of “activities of daily living” (Deacon, 2012; Jirkof, 2014), we propose they could be useful as correlates of negative symptoms,

namely avolition (Strauss et al., 2021), which are difficult to study in schizophrenia research models (Guerrin et al., 2021).

Surprisingly, CX3CR1 absence and neonatal NMDA antagonism induced broad but opposing changes in the spectral components of hippocampal LFP accompanied by respective alterations in seizure susceptibility. Both are related to alterations in the excitation/inhibition balance as neonatal NMDA blockade induces long-lasting reductions in interneuron population and molecular markers of GABAergic transmission (Coleman et al., 2009; Jones et al., 2014; Li et al., 2015). On the other hand, CX3CR1 induces an inverse shift in the LFP power spectrum, partially reversing the MK-801 effect and preventing the increase in mortality to PTZ-induced seizures. However, this does not necessarily mean a restoration of normal neural circuit physiology, but rather a fortunate coincidence, as our results (Méndez-Salcido et al., 2022) and others (Hoshiko et al., 2012; Zhan et al., 2014) indicate that CX3CR1 depletion is associated with widespread glutamatergic synaptic dysfunction and concomitant cognitive impairments.

Whether CX3CR1 absence prevents the aforementioned effects of neonatal MK-801 on the GABAergic system or only partially restores the excitation/inhibition balanced by damaging the glutamatergic system remains to be assessed. Notably, the changes in LFP and seizure-related mortality were more prominent in the low-dose group, rather than in the high-dose group, suggesting an inverted U effect of NMDA antagonism during development not recognized before.

Our results show a wide range of evidence supporting the potential role of alterations in the fractalkine pathway as a diathetic factor in neurodevelopmental models of psychiatric disorders and its interaction with neonatal NMDA antagonism as an interesting novel model to study the etiopathology and potential treatments of schizophrenic disorders with converging elements from the neurodevelopmental, glutamatergic, and neuroinflammatory hypotheses.

Declarations

Acknowledgments

We would like to thank Alejandra Castilla León and María Antonieta Carbajo Mata for their assistance and training in rodent colony management, pup handling and drug administration; Deisy Gasca Martínez for her assistance and training in behavioral tasks; Elsa Nydia Hernández Ríos and Ericka A. de los Ríos Arellano for their assistance and instruction with histological and microscopy techniques.

FAMS and MITF are students of Programa de Doctorado en Ciencias Biomédicas at Universidad Nacional Autónoma de México (UNAM) supported by Consejo Nacional de Ciencia y Tecnología (CONACyT) fellowships (ID 570426 and 629550, respectively). This work was supported by the Dirección General de Asuntos del Personal Académico, Universidad Nacional Autónoma de México, Mexico (grant number IG200521) and by CONACyT (grant number A1-S-7540), Mexico.

Funding

This work was supported by the Dirección General de Asuntos del Personal Académico, Universidad Nacional Autónoma de México (UNAM) (grant number: IG200521) and by Consejo Nacional de Ciencia y Tecnología (CONACyT) graduate studies fellowships (ID 570426 and 629550) and grant (A1-S-7540).

Competing Interests

The authors declare no conflicts of interest.

Availability of data and material

Data related to this work are available upon request to the corresponding author.

Code availability

Custom code related to the processing and analysis of the data in the present work is available in the public repository of the first author at: https://github.com/FMendezSlc/NeuroPy.

Authors' Contributions

Felipe A. Méndez: Conceptualization, methodology, software, formal analysis, investigation, writing – original draft, visualization; Mayra Itzel Torres-Flores: Conceptualization, methodology, investigation, data curation, writing – review & editing; Benito Ordaz: Investigation, data curation, writing – review and editing; Fernando Peña-Ortega: Conceptualization, supervision, resources, funding acquisition, writing – review and editing.

Ethics Approval

All experimental protocols were conducted in accordance with current Mexican regulations (NOM-062-ZOO-1999) and approved by the Bioethics Committee of the Institute of Neurobiology, UNAM.

Consent to participate

Not applicable.

Consent to publication

Not applicable.

References

1. Adler, L. E., Rose, G., & Freedman, R. (1986). Neurophysiological studies of sensory gating in rats: Effects of amphetamine, phencyclidine, and haloperidol. *Biological Psychiatry*, *21*(8–9), 787–798. https://doi.org/10.1016/0006-3223(86)90244-1
2. Arnoux, I., & Audinat, E. (2015). Fractalkine signaling and microglia functions in the developing brain. *Neural Plasticity*, *2015*. https://doi.org/10.1155/2015/689404

3. Bell, A. (2013). Randomized or fixed order for studies of behavioral syndromes? *Behavioral Ecology*, *24*(1), 16–20. https://doi.org/10.1093/beheco/ars148
4. Bessis, A., Béchade, C., Bernard, D., & Roumier, A. (2007). Microglial control of neuronal death and synaptic properties. *Glia*, *55*(3), 233–238. https://doi.org/10.1002/glia.20459
5. Bloomfield, P. S., Selvaraj, S., Veronese, M., Rizzo, G., Bertoldo, A., Owen, D. R., Bloomfield, M. A. P., Bonoldi, I., Kalk, N., Turkheimer, F., McGuire, P., de Paola, V., & Howes, O. D. (2016). Microglial Activity in People at Ultra High Risk of Psychosis and in Schizophrenia: An [11C]PBR28 PET Brain Imaging Study. *American Journal of Psychiatry*, *173*(1), 44–52. https://doi.org/10.1176/appi.ajp.2015.14101358
6. Braff, L., & Braff, D. L. (2013). The Neuropsychiatric Translational Revolution Still Very Early and Still Very Challenging. *JAMA Psychiatry*, *70*(8), 777–779. https://doi.org/10.1001/jamapsychiatry.2013.2184
7. Cardona, A. E., Pioro, E. P., Sasse, M. E., Kostenko, V., Cardona, S. M., Dijkstra, I. M., Huang, D. R., Kidd, G., Dombrowski, S., Dutta, R., Lee, J. C., Cook, D. N., Jung, S., Lira, S. A., Littman, D. R., & Ransohoff, R. M. (2006). Control of microglial neurotoxicity by the fractalkine receptor. *Nature Neuroscience*, *9*(7), 917–924. https://doi.org/10.1038/nn1715
8. Clement, E. A., Richard, A., Thwaites, M., Ailon, J., Peters, S., & Dickson, C. T. (2008). Cyclic and sleep-like spontaneous alternations of brain state under urethane anesthesia. *PLoS ONE*, *3*(4). https://doi.org/10.1371/journal.pone.0002004
9. Coleman, L. G., Jarskog, L. F., Moy, S. S., & Crews, F. T. (2009). Deficits in adult prefrontal cortex neurons and behavior following early post-natal NMDA antagonist treatment. *Pharmacology Biochemistry and Behavior*, *93*(3), 322–330. https://doi.org/10.1016/j.pbb.2009.04.017
10. Deacon, R. (2012). Assessing Burrowing, Nest Construction, and Hoarding in Mice. *J. Vis. Exp*, *59*, 2607. https://doi.org/10.3791/2607
11. Deacon, R. M. J. (2006a). Assessing nest building in mice. *Nature Protocols*, *1*(3), 1117–1119. https://doi.org/10.1038/nprot.2006.170
12. Deacon, R. M. J. (2006b). Burrowing in rodents: A sensitive method for detecting behavioral dysfunction. *Nature Protocols*, *1*(1), 118–121. https://doi.org/10.1038/nprot.2006.19
13. Dissanayake, D. W. N., Zachariou, M., Marsden, C. A., & Mason, R. (2008). Auditory gating in rat hippocampus and medial prefrontal cortex: Effect of the cannabinoid agonist WIN55,212-2. *Neuropharmacology*, *55*(8), 1397–1404. https://doi.org/10.1016/j.neuropharm.2008.08.039
14. Eyo, U. B., Peng, J., Murugan, M., Mo, M., Lalani, A., Xie, P., Xu, P., Margolis, D. J., & Wu, L.-J. (2016). Regulation of Physical Microglia–Neuron Interactions by Fractalkine Signaling after Status Epilepticus. *ENeuro*, *3*(6). https://doi.org/10.1523/ENEURO.0209-16.2016
15. Feigenson, K. A., Kusnecov, A. W., & Silverstein, S. M. (2014). Inflammation and the Two-Hit Hypothesis of Schizophrenia. *Neuroscience and Biobehavioral Reviews*, *38*, 72–93. https://doi.org/10.1016/j.neubiorev.2013.11.006

16. Feinberg, I. (1982). Schizophrenia: Caused by a fault in programmed synaptic elimination during adolescence? *Journal of Psychiatric Research*, *17*(4), 319–334. https://doi.org/10.1016/0022-3956(82)90038-3
17. Fredriksson, A., & Archer, T. (2004). Neurobehavioral deficits associated with apoptotic neurodegeneration and vulnerability for ADHD. *Neurotoxicity Research*, *6*(6), 435–456. https://doi.org/10.1007/BF03033280
18. Fries, G. R., Dimitrov, D. H., Lee, S., Braida, N., Yantis, J., Honaker, C., Cuellar, J., & Walss-Bass, C. (2018). Genome-wide expression in veterans with schizophrenia further validates the immune hypothesis for schizophrenia. *Schizophrenia Research*, *192*, 255–261. https://doi.org/10.1016/j.schres.2017.06.016
19. Goldsmith, D. R., Rapaport, M. H., & Miller, B. J. (2016). A meta-analysis of blood cytokine network alterations in psychiatric patients: Comparisons between schizophrenia, bipolar disorder and depression. *Molecular Psychiatry*, *21*(12), Article 12. https://doi.org/10.1038/mp.2016.3
20. Gorter, J. A., Titulaer, M., Bos, N. P. A., & Huisman, E. (1991). Chronic neonatal MK-801 administration leads to a long-lasting increase in seizure sensitivity during the early stages of hippocampal kindling. *Neuroscience Letters*, *134*(1), 29–32. https://doi.org/10.1016/0304-3940(91)90501-J
21. Guerrin, C. G. J., Doorduin, J., Sommer, I. E., & de Vries, E. F. J. (2021). The dual hit hypothesis of schizophrenia: Evidence from animal models. *Neuroscience & Biobehavioral Reviews*, *131*, 1150–1168. https://doi.org/10.1016/j.neubiorev.2021.10.025
22. Hansen, H. H., Briem, T., Dzietko, M., Sifringer, M., Voss, A., Rzeski, W., Zdzisinska, B., Thor, F., Heumann, R., Stepulak, A., Bittigau, P., & Ikonomidou, C. (2004). Mechanisms leading to disseminated apoptosis following NMDA receptor blockade in the developing rat brain. *Neurobiology of Disease*, *16*(2), 440–453. https://doi.org/10.1016/j.nbd.2004.03.013
23. Heck, N., Golbs, A., Riedemann, T., Sun, J. J., Lessmann, V., & Luhmann, H. J. (2008). Activity-dependent regulation of neuronal apoptosis in neonatal mouse cerebral cortex. *Cerebral Cortex*, *18*(6), 1335–1349. https://doi.org/10.1093/cercor/bhm165
24. Hoshiko, M., Arnoux, I., Avignone, E., Yamamoto, N., & Audinat, E. (2012). Deficiency of the Microglial Receptor CX3CR1 Impairs Postnatal Functional Development of Thalamocortical Synapses in the Barrel Cortex. *Journal of Neuroscience*, *32*(43), 15106–15111. https://doi.org/10.1523/JNEUROSCI.1167-12.2012
25. Howes, O. D., & McCutcheon, R. (2017). Inflammation and the neural diathesis-stress hypothesis of schizophrenia: A reconceptualization. *Translational Psychiatry*, *7*(2), Article 2. https://doi.org/10.1038/tp.2016.278
26. Howes, O. D., McCutcheon, R., Owen, M. J., & Murray, R. M. (2017). The Role of Genes, Stress, and Dopamine in the Development of Schizophrenia. *Biological Psychiatry*, *81*(1), 9–20. https://doi.org/10.1016/j.biopsych.2016.07.014
27. Howes, O. D., & Shatalina, E. (2022). Integrating the Neurodevelopmental and Dopamine Hypotheses of Schizophrenia and the Role of Cortical Excitation-Inhibition Balance. *Biological Psychiatry*, *92*(6),

501–513. https://doi.org/10.1016/j.biopsych.2022.06.017

28. Ikonomidou, C., Bosch, F., Miksa, M., Bittigau, P., Vöckler, J., Dikranian, K., Tenkova, T. I., Stefovska, V., Turski, L., & Olney, J. W. (1999). Blockade of NMDA receptors and apoptotic neurodegeneration in the developing brain. *Science*, *283*(5398), 70–74. https://doi.org/10.1126/science.283.5398.70
29. Inta, D., Lang, U. E., Borgwardt, S., Meyer-Lindenberg, A., & Gass, P. (2017). Microglia Activation and Schizophrenia: Lessons From the Effects of Minocycline on Postnatal Neurogenesis, Neuronal Survival and Synaptic Pruning. *Schizophrenia Bulletin*, *43*(3), 493–496. https://doi.org/10.1093/schbul/sbw088
30. Jirkof, P. (2014). Burrowing and nest building behavior as indicators of well-being in mice. *Journal of Neuroscience Methods*, *234*, 139–146. https://doi.org/10.1016/j.jneumeth.2014.02.001
31. Jones, K. S., Corbin, J. G., & Huntsman, M. M. (2014). Neonatal NMDA Receptor Blockade Disrupts Spike Timing and Glutamatergic Synapses in Fast Spiking Interneurons in a NMDA Receptor Hypofunction Model of Schizophrenia. *PLOS ONE*, *9*(10), e109303. https://doi.org/10.1371/journal.pone.0109303
32. Jung, S., Aliberti, J., Graemmel, P., Sunshine, M. J., Kreutzberg, G. W., Sher, A., & Littman, D. R. (2000). Analysis of Fractalkine Receptor CX3CR1 Function by Targeted Deletion and Green Fluorescent Protein Reporter Gene Insertion. *Molecular and Cellular Biology*, *20*(11), 4106–4114. https://doi.org/10.1128/MCB.20.11.4106-4114.2000
33. Keshavan, M. S., Anderson, S., & Pettegrew, J. W. (1994). Is schizophrenia due to excessive synaptic pruning in the prefrontal cortex? The Feinberg hypothesis revisited. *Journal of Psychiatric Research*, *28*(3), 239–265. https://doi.org/10.1016/0022-3956(94)90009-4
34. Kraeuter, A.-K., Guest, P. C., & Sarnyai, Z. (2019). The Y-Maze for Assessment of Spatial Working and Reference Memory in Mice. *Methods in Molecular Biology (Clifton, N.J.)*, *1916*, 105–111. https://doi.org/10.1007/978-1-4939-8994-2_10
35. Kramis, R., Vanderwolf, C. H., & Bland, B. H. (1975). Two types of hippocampal rhythmical slow activity in both the rabbit and the rat: Relations to behavior and effects of atropine, diethyl ether, urethane, and pentobarbital. *Experimental Neurology*, *49*(1), 58–85. https://doi.org/10.1016/0014-4886(75)90195-8
36. Krause, M., Hoffmann, W. E., & Hajós, M. (2003). Auditory sensory gating in hippocampus and reticular thalamic neurons in anesthetized rats. *Biological Psychiatry*, *53*(3), 244–253. https://doi.org/10.1016/S0006-3223(02)01463-4
37. Lee, G., & Zhou, Y. (2019). NMDAR Hypofunction Animal Models of Schizophrenia. *Frontiers in Molecular Neuroscience*, *12*. https://doi.org/10.3389/fnmol.2019.00185
38. Li, J.-T., Zhao, Y.-Y., Wang, H.-L., Wang, X.-D., Su, Y.-A., & Si, T.-M. (2015). Long-term effects of neonatal exposure to MK-801 on recognition memory and excitatory–inhibitory balance in rat hippocampus. *Neuroscience*, *308*, 134–143. https://doi.org/10.1016/j.neuroscience.2015.09.003
39. Lim, A. L., Taylor, D. A., & Malone, D. T. (2012). Consequences of early life MK-801 administration: Long-term behavioral effects and relevance to schizophrenia research. *Behavioural Brain Research*,

227, 276–286. https://doi.org/10.1016/j.bbr.2011.10.052

40. McIlwain, K. L., Merriweather, M. Y., Yuva-Paylor, L. A., & Paylor, R. (2001). The use of behavioral test batteries: Effects of training history. *Physiology & Behavior*, *73*(5), 705–717. https://doi.org/10.1016/s0031-9384(01)00528-5
41. Méndez-Salcido, F. A., Torres-Flores, M. I., Ordaz, B., & Peña-Ortega, F. (2022). Abnormal innate and learned behavior induced by neuron–microglia miscommunication is related to CA3 reconfiguration. *Glia*, *70*(9), 1630–1651. https://doi.org/10.1002/glia.24185
42. Milior, G., Lecours, C., Samson, L., Bisht, K., Poggini, S., Pagani, F., Deflorio, C., Lauro, C., Alboni, S., Limatola, C., Branchi, I., Tremblay, M.-E., & Maggi, L. (2016). Fractalkine receptor deficiency impairs microglial and neuronal responsiveness to chronic stress. *Brain, Behavior, and Immunity*, *55*, 114–125. https://doi.org/10.1016/j.bbi.2015.07.024
43. Miller, C. L., & Freedman, R. (1995). The activity of hippocampal interneurons and pyramidal cells during the response of the hippocampus to repeated auditory stimuli. *Neuroscience*, *69*(2), 371–381. https://doi.org/10.1016/0306-4522(95)00249-I
44. Miyamoto, S., Duncan, G. E., Marx, C. E., & Lieberman, J. A. (2005). Treatments for schizophrenia: A critical review of pharmacology and mechanisms of action of antipsychotic drugs. *Molecular Psychiatry*, *10*(1), Article 1. https://doi.org/10.1038/sj.mp.4001556
45. Mongan, D., Ramesar, M., Föcking, M., Cannon, M., & Cotter, D. (2019). Role of inflammation in the pathogenesis of schizophrenia: A review of the evidence, proposed mechanisms and implications for treatment. *Early Intervention in Psychiatry*, eip.12859. https://doi.org/10.1111/eip.12859
46. Montgomery, S. M., Sirota, A., & Buzsáki, G. (2008). Theta and Gamma Coordination of Hippocampal Networks during Waking and Rapid Eye Movement Sleep. *Journal of Neuroscience*, *28*(26), 6731–6741. https://doi.org/10.1523/JNEUROSCI.1227-08.2008
47. Multivariate Analysis of Variance (MANOVA). (2010). In N. Salkind, *Encyclopedia of Research Design*. SAGE Publications, Inc. https://doi.org/10.4135/9781412961288.n257
48. Murray, R. M., Bhavsar, V., Tripoli, G., & Howes, O. (2017). 30 Years on: How the Neurodevelopmental Hypothesis of Schizophrenia Morphed Into the Developmental Risk Factor Model of Psychosis. *Schizophrenia Bulletin*, *43*(6), 1190–1196. https://doi.org/10.1093/schbul/sbx121
49. Nakazawa, K., Jeevakumar, V., & Nakao, K. (2017). Spatial and temporal boundaries of NMDA receptor hypofunction leading to schizophrenia. *Npj Schizophrenia*, *3*(1), Article 1. https://doi.org/10.1038/s41537-016-0003-3
50. Owen, M. J., O'Donovan, M. C., Thapar, A., & Craddock, N. (2011). Neurodevelopmental hypothesis of schizophrenia. *The British Journal of Psychiatry*, *198*(3), 173–175. https://doi.org/10.1192/bjp.bp.110.084384
51. Pagani, F., Paolicelli, R. C., Murana, E., Cortese, B., Di Angelantonio, S., Zurolo, E., Guiducci, E., Ferreira, T. a, Garofalo, S., Catalano, M., D'Alessandro, G., Porzia, A., Peruzzi, G., Mainiero, F., Limatola, C., Gross, C. T., & Ragozzino, D. (2015). Defective microglial development in the hippocampus of Cx3cr1

deficient mice. *Frontiers in Cellular Neuroscience*, *9*(March), 111. https://doi.org/10.3389/fncel.2015.00111

52. Paolicelli, R. C., Bisht, K., & Tremblay, M. (2014). Fractalkine regulation of microglial physiology and consequences on the brain and behavior. *Frontiers in Cellular Neuroscience*, *8*(May), 1–10. https://doi.org/10.3389/fncel.2014.00129
53. Paolicelli, R. C., Bolasco, G., Pagani, F., Maggi, L., Scianni, M., Panzanelli, P., Giustetto, M., Ferreira, T. A., Guiducci, E., Dumas, L., Ragozzino, D., & Gross, C. T. (2011). Synaptic pruning by microglia is necessary for normal brain development. *Science (New York, N.Y.)*, *333*(6048), 1456–1458. https://doi.org/10.1126/science.1202529
54. Paul, C. A., Beltz, B., & Berger-Sweeney, J. (2008). The Nissl Stain: A Stain for Cell Bodies in Brain Sections. *Cold Spring Harbor Protocols*, *2008*(9), pdb.prot4805. https://doi.org/10.1101/pdb.prot4805
55. Peña, F., Ordaz, B., Balleza-Tapia, H., Bernal-Pedraza, R., Márquez-Ramos, A., Carmona-Aparicio, L., & Giordano, M. (2010). Beta-amyloid protein (25–35) disrupts hippocampal network activity: Role of Fyn-kinase. *Hippocampus*, *20*(1), 78–96. https://doi.org/10.1002/hipo.20592
56. Pierson, M., & Swann, J. (1991). Sensitization to noise-mediated induction of seizure susceptibility by MK-801 and phencyclidine. *Brain Research*, *560*(1), 229–236. https://doi.org/10.1016/0006-8993(91)91237-U
57. Réus, G. Z., Fries, G. R., Stertz, L., Badawy, M., Passos, I. C., Barichello, T., Kapczinski, F., & Quevedo, J. (2015). The role of inflammation and microglial activation in the pathophysiology of psychiatric disorders. *Neuroscience*, *300*, 141–154. https://doi.org/10.1016/j.neuroscience.2015.05.018
58. Rogers, J. T., Morganti, J. M., Bachstetter, A. D., Hudson, C. E., Peters, M. M., Grimmig, B. A., Weeber, E. J., Bickford, P. C., & Gemma, C. (2011). CX3CR1 Deficiency Leads to Impairment of Hippocampal Cognitive Function and Synaptic Plasticity. *Journal of Neuroscience*, *31*(45), 16241–16250. https://doi.org/10.1523/JNEUROSCI.3667-11.2011
59. Salgado-Puga, K., Prado-Alcalá, R. A., & Peña-Ortega, F. (2015). Amyloid β Enhances Typical Rodent Behavior While It Impairs Contextual Memory Consolidation. *Behavioural Neurology*, *2015*. https://doi.org/10.1155/2015/526912
60. Schindelin, J., Arganda-Carreras, I., Frise, E., Kaynig, V., Longair, M., Pietzsch, T., Preibisch, S., Rueden, C., Saalfeld, S., Schmid, B., Tinevez, J.-Y., White, D. J., Hartenstein, V., Eliceiri, K., Tomancak, P., & Cardona, A. (2012). Fiji: An open-source platform for biological-image analysis. *Nature Methods*, *9*(7), 676–682. https://doi.org/10.1038/nmeth.2019
61. Seibenhener, M. L., & Wooten, M. C. (2015). Use of the open field maze to measure locomotor and anxiety-like behavior in mice. *Journal of Visualized Experiments*, *96*. https://doi.org/10.3791/52434
62. Sellgren, C. M., Gracias, J., Watmuff, B., Biag, J. D., Thanos, J. M., Whittredge, P. B., Fu, T., Worringer, K., Brown, H. E., Wang, J., Kaykas, A., Karmacharya, R., Goold, C. P., Sheridan, S. D., & Perlis, R. H. (2019). Increased synapse elimination by microglia in schizophrenia patient-derived models of synaptic pruning. *Nature Neuroscience*, *22*(3), Article 3. https://doi.org/10.1038/s41593-018-0334-7

63. Shimada, T., & Yamagata, K. (2018). Pentylenetetrazole-Induced Kindling Mouse Model. *JoVE (Journal of Visualized Experiments)*, *136*, e56573. https://doi.org/10.3791/56573
64. Smucny, J., Stevens, K. E., Olincy, A., & Tregellas, J. R. (2015). Translational utility of rodent hippocampal auditory gating in schizophrenia research: A review and evaluation. *Translational Psychiatry*, *5*(6), e587–e587. https://doi.org/10.1038/tp.2015.77
65. Strauss, G. P., Bartolomeo, L. A., & Harvey, P. D. (2021). Avolition as the core negative symptom in schizophrenia: Relevance to pharmacological treatment development. *Npj Schizophrenia*, *7*(1), Article 1. https://doi.org/10.1038/s41537-021-00145-4
66. Strauss, G. P., Whearty, K. M., Morra, L. F., Sullivan, S. K., Ossenfort, K. L., & Frost, K. H. (2016). Avolition in schizophrenia is associated with reduced willingness to expend effort for reward on a progressive ratio task. *Schizophrenia Research*, *170*(1), 198–204. https://doi.org/10.1016/j.schres.2015.12.006
67. Tapia, R., Peña, F., & Arias, C. (1999). Neurotoxic and Synaptic Effects of Okadaic Acid, an Inhibitor of Protein Phosphatases. *Neurochemical Research*, *24*(11), 1423–1430. https://doi.org/10.1023/A:1022588808260
68. Ueno, M., Fujita, Y., Tanaka, T., Nakamura, Y., Kikuta, J., Ishii, M., & Yamashita, T. (2013). Layer v cortical neurons require microglial support for survival during postnatal development. *Nature Neuroscience*, *16*(5), 543–551. https://doi.org/10.1038/nn.3358
69. van Berckel, B. N., Bossong, M. G., Boellaard, R., Kloet, R., Schuitemaker, A., Caspers, E., Luurtsema, G., Windhorst, A. D., Cahn, W., Lammertsma, A. A., & Kahn, R. S. (2008). Microglia Activation in Recent-Onset Schizophrenia: A Quantitative (R)-[11C]PK11195 Positron Emission Tomography Study. *Biological Psychiatry*, *64*(9), 820–822. https://doi.org/10.1016/j.biopsych.2008.04.025
70. Van Eden, C. G., & Uylings, H. B. (1985). Cytoarchitectonic development of the prefrontal cortex in the rat. *The Journal of Comparative Neurology*, *241*(3), 253–267. https://doi.org/10.1002/cne.902410302
71. Van Erum, J., Van Dam, D., & De Deyn, P. P. (2019). PTZ-induced seizures in mice require a revised Racine scale. *Epilepsy & Behavior*, *95*, 51–55. https://doi.org/10.1016/j.yebeh.2019.02.029
72. Vandecasteele, M., Varga, V., Berényi, A., Papp, E., Barthó, P., Venance, L., Freund, T. F., & Buzsáki, G. (2014). Optogenetic activation of septal cholinergic neurons suppresses sharp wave ripples and enhances theta oscillations in the hippocampus. *Proceedings of the National Academy of Sciences*, *111*(37), 13535–13540. https://doi.org/10.1073/pnas.1411233111
73. Venable, N., & Kelly, P. H. (1990). Effects of NMDA receptor antagonists on passive avoidance learning and retrieval in rats and mice. *Psychopharmacology*, *100*(2), 215–221. https://doi.org/10.1007/BF02244409
74. Yona, S., Kim, K.-W., Wolf, Y., Mildner, A., Varol, D., Breker, M., Strauss-Ayali, D., Viukov, S., Guilliams, M., Misharin, A., Hume, D. A., Perlman, H., Malissen, B., Zelzer, E., & Jung, S. (2013). Fate mapping reveals origins and dynamics of monocytes and tissue macrophages under homeostasis. *Immunity*, *38*(1), 79–91. https://doi.org/10.1016/j.immuni.2012.12.001

75. Zhan, Y., Paolicelli, R. C., Sforazzini, F., Weinhard, L., Bolasco, G., Pagani, F., Vyssotski, A. L., Bifone, A., Gozzi, A., Ragozzino, D., & Gross, C. T. (2014). Deficient neuron-microglia signaling results in impaired functional brain connectivity and social behavior. *Nature Neuroscience*, *17*(3), 400–406. https://doi.org/10.1038/nn.3641

Figures

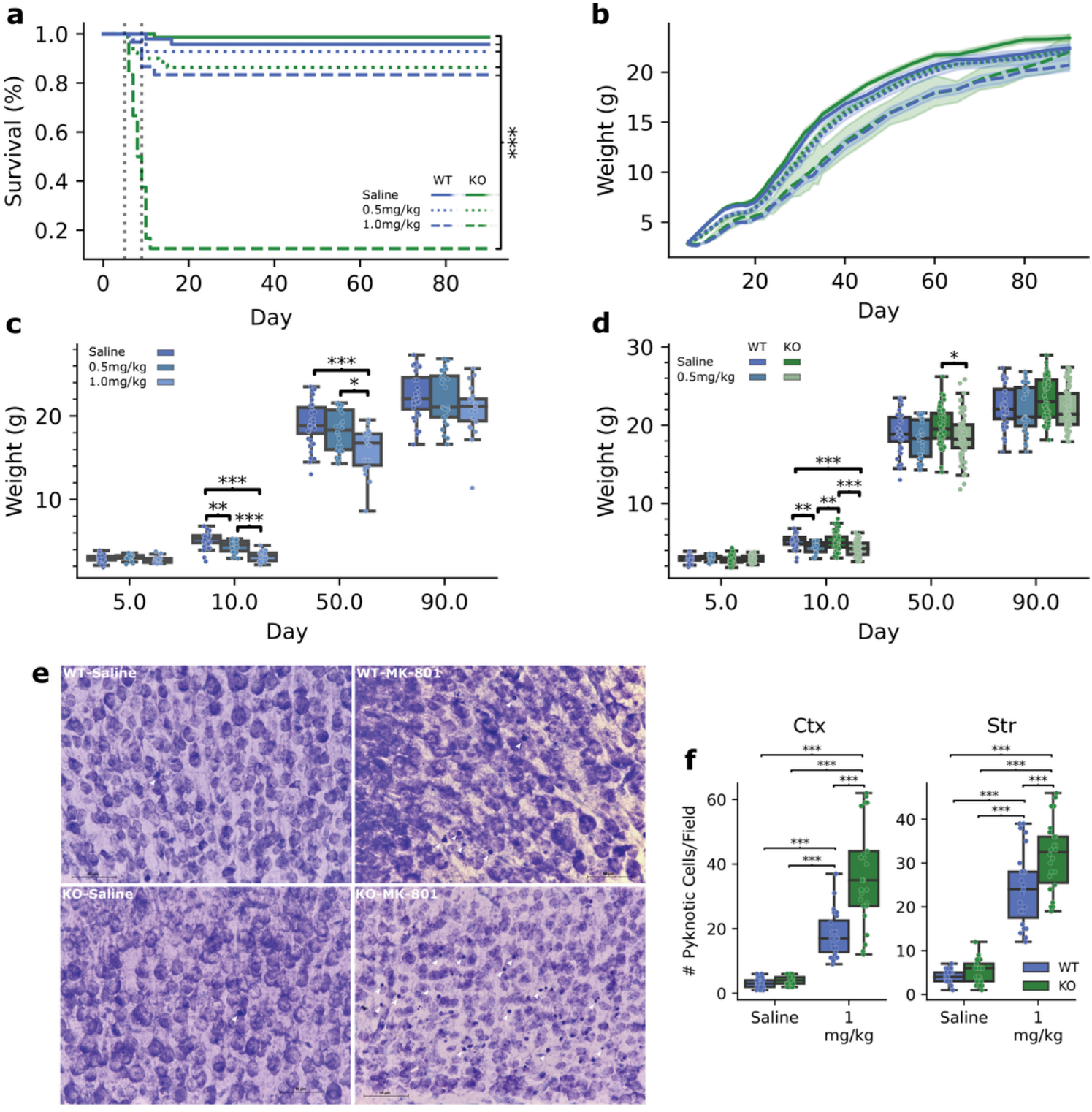

Figure 1

Synergism of NMDA antagonism and Cx3cr1 absence on neuronal apoptosis and mortality

a) Survival curves during the neonatal MK-801 administration protocol. Cx3cr1 absence (KO) abruptly increases the mortality of the high dose (1 mg/kg) of MK-801 (Tab. 1). **b)** Weight gain during the neonatal MK-801 administration protocol. NMDA antagonism induced a dose-dependent delay in the growth of Cx3cr1 wild-type (WT) mice, with moderate to big effect sizes during development, that normalizes in adulthood; **c)** Comparisons of weight gain during the neonatal MK-801 administration protocol in WT animals (mixed-model ANOVA). Treatment x Day: [F (6, 243) = 4.43, p = 0.0003], n= 26-36; Holm's corrected T-tests: P10 WT-Saline vs WT-0.5mg/kg: t_{59} = 3.75, p = 0.004, Hedges' g = 0.92; P10 WT-Saline vs WT-1mg/kg: t_{55} = 10.00, p < 0.001, Hedges' g = 2.44; P50 WT-Saline vs WT-0.5mg/kg: t_{55} = 1.34, p = 0.61, Hedges' g = 0.33; P50 WT-Saline vs WT-1mg/kg: $t_{43.23}$ = 4.42, p = 0.0006, Hedges' g = 1.19). This effect was not exacerbated in the KO group; **d)** Comparisons of weight gain during the neonatal MK-801 administration protocol in WT and KO animals (mixed-model ANOVA). Group x Day: [F (9, 570) = 3.90, p < 0.0001], n= 26-68; Holm's corrected T-tests: P10 WT-Saline vs WT-0.5mg/kg: t59 = 3.75, p = 0.008, Hedges' g = 0.92; P10 WT-Saline vs KO-0.5mg/kg: t73.96 = 4.99, p < 0.0001, Hedges' g = 1.02; P10 KO-Saline vs WT-0.5mg/kg: t64.75 = 3.75, p = 0.008, Hedges' g = 0.73; P10 KO-Saline vs KO-0.5mg/kg: t129.27 = 5.16, p < 0.0001, Hedges' g = 0.89; P50 KO-Saline vs KO-0.5mg/kg: t123.26 = 3.12, p = 0.04, Hedges' g = 0.54). **e-f)** Apoptosis evaluation after three MK-801 administrations. Cx3cr1 depletion drastically increased MK-801 induced neuronal apoptosis in the cortex (Ctx), (Two-way ANOVA; Genotype x Treatment: [F (1, 1) = 26.45, p < 0.0001], Tukey HSD: WT-1mg/kg vs KO-1mg/kg, p = 0.001, Hedges' g = 2.13) and in the striatum (Str), (Two-way ANOVA; Genotype x Treatment: [F (1, 1) = 7.19, p = 0.008], Tukey HSD: WT-1mg/kg vs KO-1mg/kg, p = 0.001, Hedges' g = 1.22, n = 23-27, 3 mice per group).

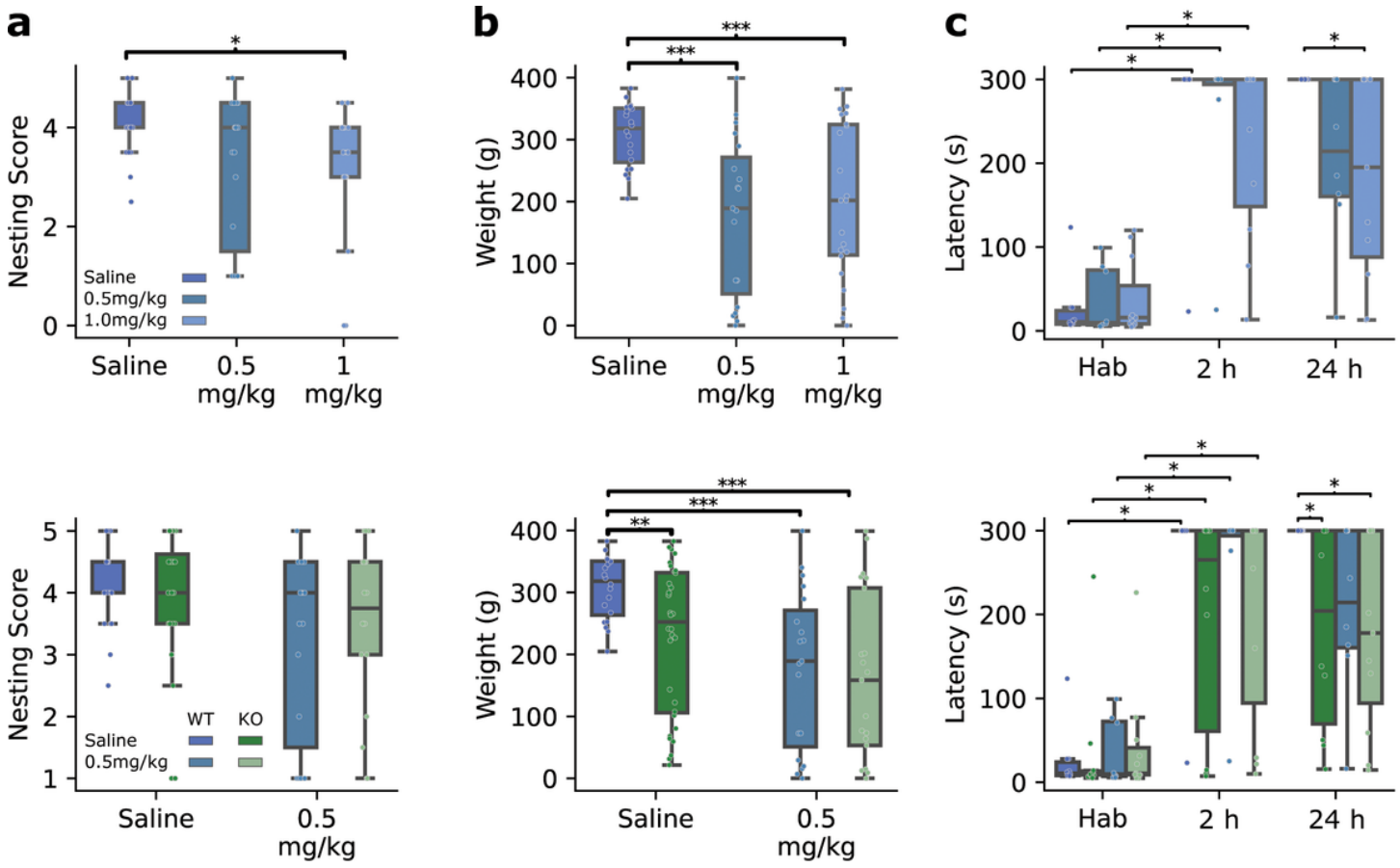

Figure 2

NMDA antagonism and Cx3cr1 absence independently impair innate behaviors and contextual memory

a) Nesting test. Nesting building was affected by neonatal MK-801 treatment in a dose-dependent manner in Cx3cr1 wild-type (WT) mice; **Top**, Kruskal–Wallis, H(2) = 8.56, p = 0.01; post-hoc Dunn test, WT-Saline vs WT-0.5mg/kg, p = 0.1, WT-Saline vs WT-1mg/kg, p = 0.014, n=19-26. This impairment did not worsen by Cx3cr1 absence (KO); **Bottom,** Kruskal–Wallis, H(3) = 4.04, p = 0.26, 19-32. **b)** Burrowing test. Burrowing was affected by Cx3cr1 absence and NMDA antagonism significantly but independently. Both dosages had a similar effect in WT mice; **Top**, Welch ANOVA; Treatment [F (2) = 13.17, p < 0.0001], post hoc Games–Howell, WT-Saline vs WT-0.5mg/kg: p = 0.001, Hedges' g = 1.29, WT-Saline vs WT-1mg/kg: p = 0.001, Hedges' g = 1.12, n= 19-23. In KO mice NMDA antagonism and Cx3cr1 absence had moderate to big effects without additional interaction, **Bottom,** Welch ANOVA; Group [F (3) = 12.43, p < 0.0001], post hoc Games-Howell; WT-Saline vs KO-Saline: p = 0.004, Hedges' g = 0.97, WT-Saline vs WT-0.5mg/kg: p = 0.001, Hedges' g = 1.30; WT-Saline vs KO-0.5mg/kg: p = 0.001, Hedges' g = 1.40, n=19-32. **c)** Passive avoidance test. A dose-dependent recall impairment of contextual memory is induced in WT mice, **Top**, Kruskal–Wallis, H(2) = 8.39, p = 0.015, post hoc Dunn test, WT-Saline vs WT-0.5mg/kg, p = 0.06, WT-Saline vs WT-1mg/kg, p = 0.02. In comparison, there is a primary impairment in the KO mice that did not worsen by the pharmacological treatment, **Bottom**, Kruskal–Wallis, H(3) = 10.15, p = 0.017, post hoc Dunn test; WT-Saline vs KO-Saline, p = 0.04, WT-Saline vs KO-0.5mg/kg, p = 0.03.

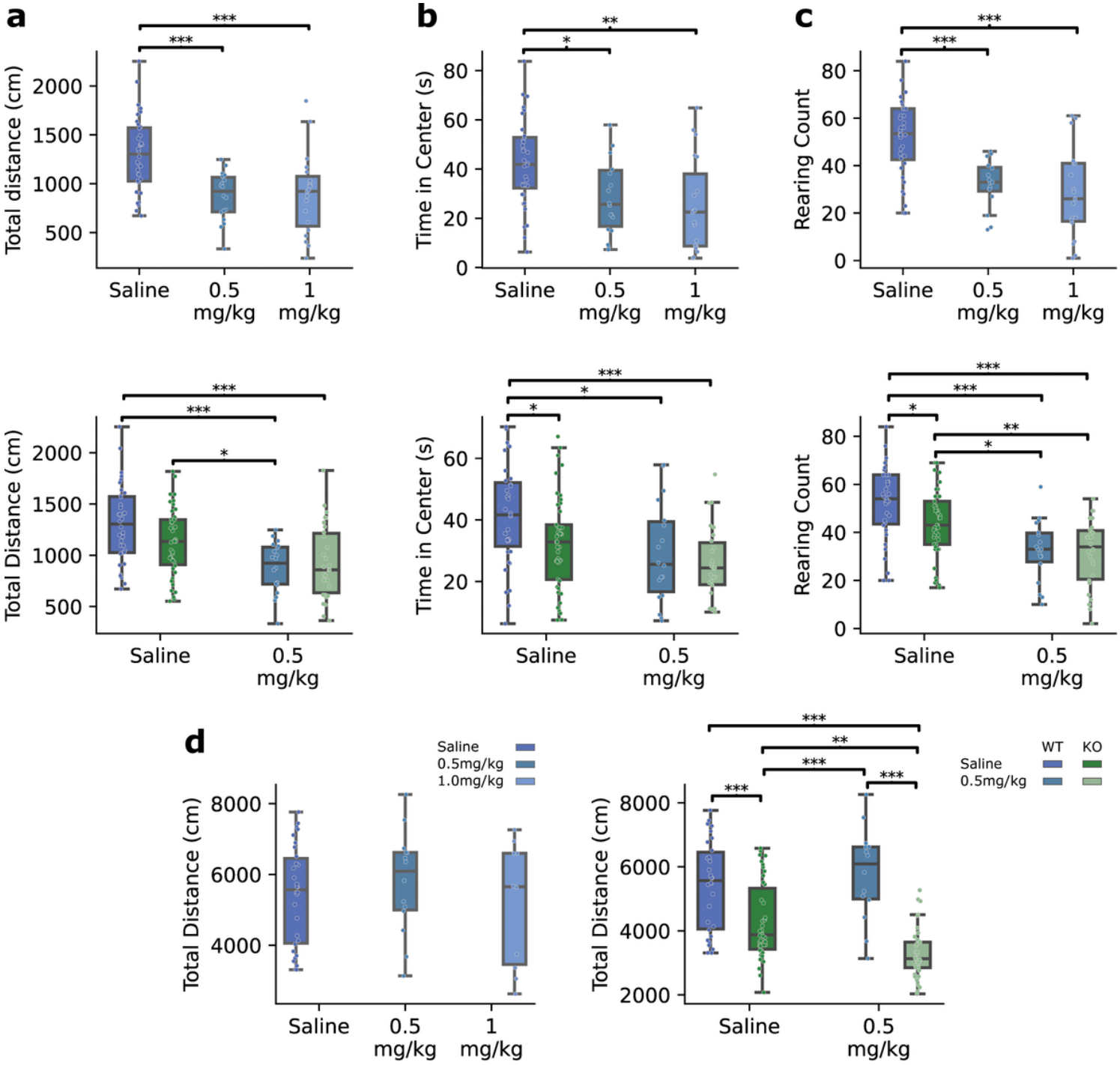

Figure 3

Neonatal NMDA antagonism and Cx3cr1 absence increase trait-anxiety and blunt spatial exploration

a-c) Open field test. **Top** Neonatal administration of MK-801 significantly increased anxiety-like behavior in Cx3cr1wildtype (WT) mice in the open field as suggested by a diminished total distance explored (**a,** One-way ANOVA: Treatment, [$F(2, 73) = 13.51$, $p < 0.0001$], post hoc Tukey-HSD: WT-Saline vs WT-0.5mg/kg, $p = 0.001$, Hedges' $g = 1.14$; WT-Saline vs WT-1mg/kg, $p = 0.001$, Hedges' $g = 1.21$); reduced time in the center of the arena, (**b**, One-way ANOVA: Treatment, [$F(2, 70) = 7.05$, $p = 0.001$], post hoc Tukey-HSD: WT-Saline vs WT-0.5mg/kg, $p = 0.02$, Hedges' $g = 0.75$; WT-Saline vs WT-1mg/kg, $p = 0.002$, Hedges'

g = 0.95); and interestingly abolished vertical exploration as assessed by a reduced rearing count, (**C,** One-way ANOVA: Treatment, [F(2, 68) = 17.22, p < 0.0001], post hoc Tukey-HSD: WT-Saline vs WT-0.5mg/kg, p = 0.001, Hedges' g = 1.22; WT-Saline vs WT-1mg/kg, p = 0.001, Hedges' g = 1.47, n = 20-36). **a-c) Bottom** On Cx3cr1 lacking mice (KO) the same effects from the treatment were observed with an interaction between Cx3cr1 absence and NMDA antagonism approaching significance in the total distance explored, (**a,** Two-way ANOVA; Treatment, [F (1,1) = 22.20, p < 0.0001], Genotype x Treatment: [F(1,1) = 3.57, p = 0.06]; both factors are significant in reducing the time spent in the center of the arena, although independently, (**b**, Two-way ANOVA; Genotype, [F (1,1) = 6.42, p = 0.01]; Treatment, [F (1,1) = 10.14, p = 0.002]; Genotype x Treatment [F(1,1) = 0.96, p = 0.33]); finally the same effects were observed for the reduction in rearing count, (**c**, Two-way ANOVA, Genotype [F (1,1) = 5.01, p = 0.02]; Treatment [F (1,1) = 35.09, p < 0.0001], Genotype x Treatment [F(1,1) = 1.72, p = 0.19], n = 20-46. **d)** Y maze. **Left**, While exploration in the Y maze was not affected significantly in WT mice (One-way ANOVA: Treatment [F(2,51) = 0.56, p = 0.57], n = 10-30), **Right**, Cx3cr1 depletion reduces the total distance explored by KO mice. This effect was exacerbated by the pharmacological treatment with a significant interaction, (Two-way ANOVA, Genotype [F(1) = 53.88, p < 0.0001]; Treatment [F(1) = 6.46, p = 0.01], Genotype x Treatment [F(1,1) = 8.49, p = 0.004], n = 10-52).

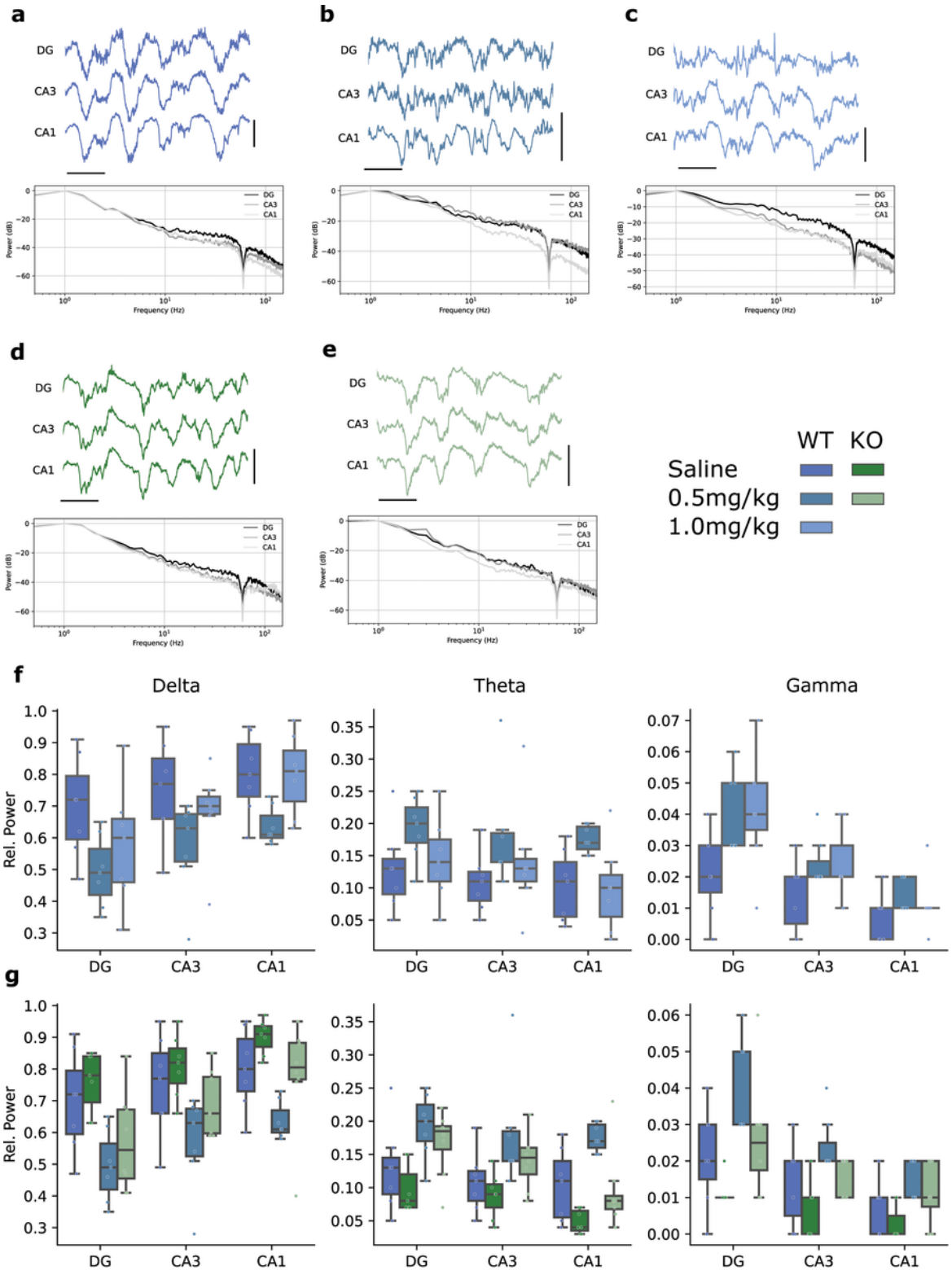

Figure 4

Neonatal NMDA antagonism and Cx3cr1 depletion induce opposed changes in the spectral composition of hippocampal LFP

a-e) Top; Representative traces of selected channels by hippocampal region and group in LFP recordings during spontaneous activity low-pass filtered at 1 kHz; scales are 100 mV and 1 s. **Bottom**, Welch

periodogram calculated over 1 min segments for each channel (scaled to dB). **f)**Changes in relative power in the delta, theta and gamma bands induced by neonatal MK-801 treatment in WT mice. MANOVA analysis indicates Treatment and Recording Site are significant factors; delta + theta + gamma ~ Treatment +Site; Lambda de Wilks = 0.0074, $p < 0.0001$; Treatment: Wilks' Lambda = 0.63, $p = 0.0003$; Site: Wilks' Lambda = 0.55, $p = 0.0001$, n= 7. Unexpectedly the low dose treatment (0.5 mg/kg) induced the greatest changes decreasing delta band power, (Two-way ANOVA, Treatment:[$F(2) = 9.02$, $p = 0.0004$], Site: [$F(2) = 6.56$, $p = 0.003$], Treatment x Site: [$F(4) = 0.37$, $p = 0.85$], post hoc Tukey-HSD; Saline vs 0.5mg/kg: $p = 0.001$, Hedges' g = 1.19; Saline vs 1mg/kg:$p = 0.36$; 0.5mg/kg vs 1mg/kg: $p = 0.03$, increasing theta band power, (Two-way ANOVA; Treatment: [$F(2) = 7.09$, $p = 0.002$], Site: [$F(2) = 1.17$, $p = 0.32$], Treatment x Site: [$F(4) = 0.22$, $p = 0.92$], post hoc Tukey-HSD; Saline vs 0.5mg/kg: $p = 0.0015$, Hedges' g = 1.11; Saline vs 1mg/kg: $p = 0.70$); 0.5mg/kg vs 1mg/kg: $p = 0.015$, Hedges' g = 0.87, and increasing gamma band power, (Two-way ANOVA: Treatment: [$F(2) = 7.27$, $p = 0.0016$], Site: [$F(2) = 21.93$, $p < 0.0001$], Treatment x Site: [$F(4) = 0.92$, $p = 0.46$], n = 7). **G)** Cx3cr1 depletion induced opposite changes, partially preventing the increase in power of higher frequency bands in the hippocampus of KO mice. MANOVA; delta + theta + gamma ~ Treatment + Site + Genotype; Wilks' Lambda = 0.0071, $p < 0.0001$, Treatment: Wilks' Lambda = 0.62, $p = 0.0001$; Site: Wilks' Lambda = 0.66, $p = 0.0001$; Genotype: Wilks' Lambda = 0.74, $p = 0.0001$, n = 7-8. Genotype increased delta band relative power while Treatment decreased it, (Three-way ANOVA: Treatment: [$F(1) = 34.26$, $p < 0.0001$], Site: [$F(2) = 10.50$, $p < 0.0001$], Genotype: [$F(1) = 12.39$, $p = 0.0007$], post hocTukey-HSD; Saline vs 0.5mg/kg: $p = 0.001$, Hedges' g = 1.09; KO vs WT: $p = 0.0096$, Hedges' g = 0.56); the inverse relationship is observed in theta, (Three-way ANOVA; Treatment: [$F(1) = 32.81$, $p < 0.0001$], Site: [$F(2) = 5.35$, $p = 0.0067$], Genotype: [$F(1) = 15.86$, $p = 0.0001$], post hoc Tukey-HSD; Saline vs 0.5mg/kg: $p = 0.001$, Hedges' g = 1.09; KO vs WT: $p = 0.0024$, Hedges' g = 0.67; and gamma bands, (Three-way ANOVA; Treatment: [$F(1) = 29.43$, $p < 0.0001$], Site: [$F(2) = 20.39$, $p = 0.0001$], Genotype: [$F(1) = 14.34$, $p = 0.0003$], post hoc Tukey-HSD; Saline vs 0.5mg/kg: $p = 0.001$, Hedges' g = 0.91; KO vs WT: $p = 0.0087$, Hedges' g = 0.57, n= 7-8.

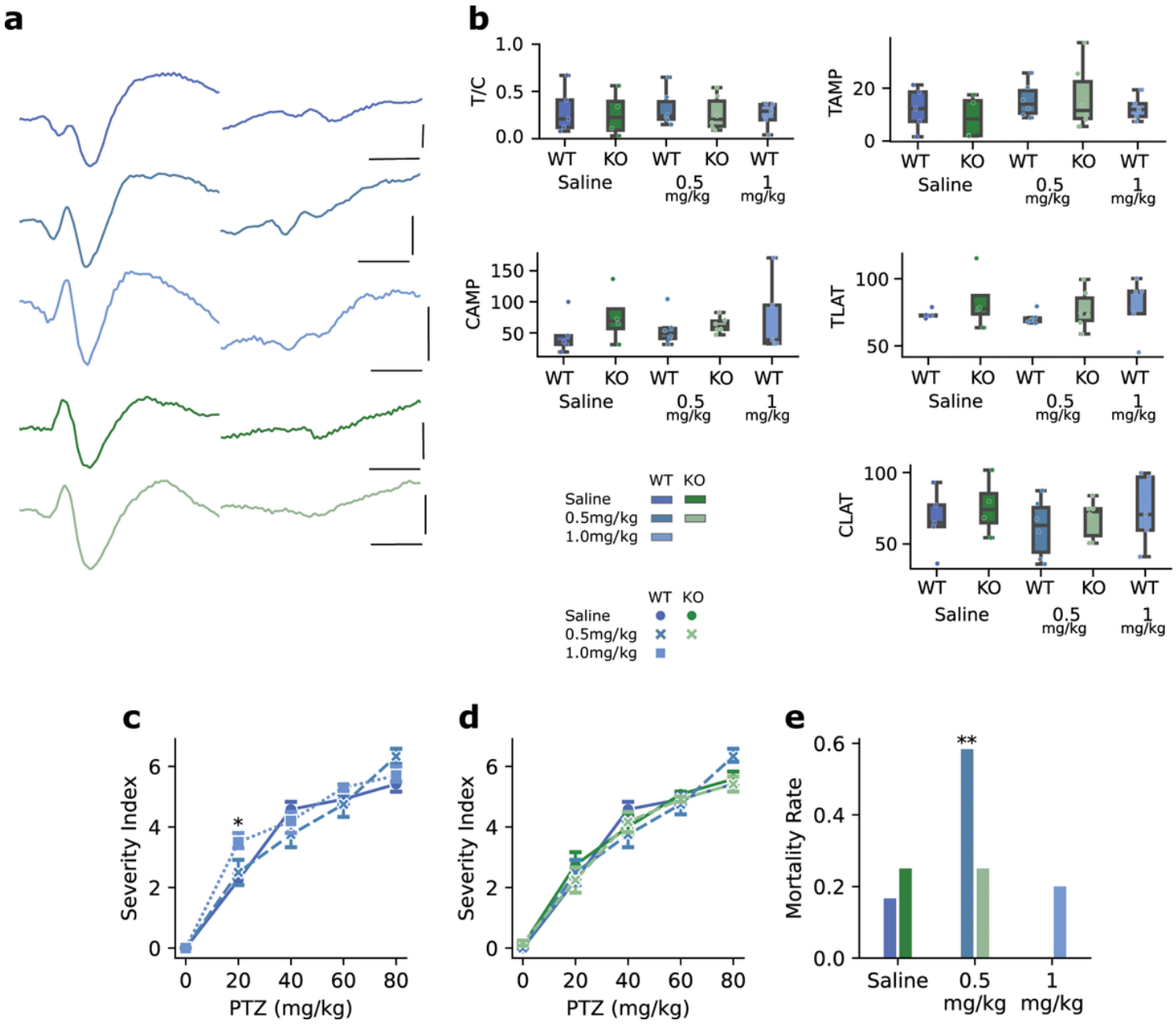

Figure 5

Cx3cr1 absence does not affect sensory gating and prevents the epileptogenic effect of MK-801 treatment

a) Representative traces of event-related potentials in the hippocampal CA3 region evoked by paired auditory stimulation. Attenuation of the second potential is preserved in all groups. **b)** All parameters of the event-related potentials remain unchanged, including: ratio of the amplitude of test potential to conditioned potential (T/C), (One-way ANOVA, [F(4,21) = 0.11, p = 0.98]); amplitude of the conditioned potential (CAMP), (One-way ANOVA, [F(4,21) = 0.56, p = 0.69]); amplitude of the test potential, (One-way ANOVA, [F(4,21) = 0.60, p = 0.66]); latency of the conditioned potential (CLAT), (One-way ANOVA, [F(4,21) = 0.43, p = 0.78]); latency of the test potential, TLAT, (One-way ANOVA, [F(4,21) = 0.59, p = 0.67], n = 4-6). **c)** High dose (1 mg/kg) MK-801 treatment increased the severity of pentylenetetrazole (PTZ) induced

seizures at the lower dose (20 mg/kg), (Mixed model ANOVA, Treatment x PTZ Dosage: [F(8,116) = 3.15, p = 0.0028], Holm's adjusted t-test; Saline vs 1 mg/kg at 20 mg/kg of PTZ: p = 0.001, n = 10-12), suggesting a reduced seizure threshold in WT mice. **d)** No significant difference in seizure severity was found among Cx3cr1 wild-type (WT) or Cx3cr1 absence (KO) groups treated with the low dose (0.5 mg/kg) of MK-801 or Saline at any dose of PTZ, (Mixed model ANOVA, Treatment x PTZ Dosage: [F(12,168) = 1.35, p = 0.19], n = 12). **e)**Low dose MK-801 treatment drastically increased the mortality of PTZ-induced seizures in WT but not KO mice, (Binomial test with Holm correction: WT-Saline vs WT-0.5mg/kg, p = 0.005). High dose MK-801 treatment did not show any increase in mortality, (Binomial test with Holm correction: WT-Saline vs WT-1mg/kg, p = 1.0).